A human immune system (HIS) mouse model that dissociates roles for mouse and human FcR + cells during antibody-mediated immune responses

Anna Louisa Thaller, Friederike Jönsson, Oriane Fiquet, Solenne Marie, Jean-marc Doisne, Giulia Girelli-Zubani, Toshiki Eri, Priyanka Fernandes, Evgeny Tatirovsky, Francina Langa Vives, et al.

European Journal of Immunology
Clinical·Basic·Translational

New Technology

Basic

Research Article

A human immune system (HIS) mouse model that dissociates roles for mouse and human FcR$^+$ cells during antibody-mediated immune responses

Anna Louisa Thaller[1], *Friederike Jönsson*[2], *Oriane Fiquet*[1], *Solenne Marie*[1], *Jean-Marc Doisne*[1], *Giulia Girelli-Zubani*[1], *Toshiki Eri*[1], *Priyanka Fernandes*[1], *Evgeny Tatirovsky*[1], *Francina Langa-Vives*[3], *Pierre Bruhns*[2], *Hélène Strick-Marchand*[*1] and *James P. Di Santo*[*1]

[1] Institut Pasteur, Innate Immunity Unit, Université Paris Cité, Inserm U1223, Paris, France
[2] Institut Pasteur, Antibodies in Therapy and Pathology Unit, Université Paris Cité, Inserm U1222, Paris, France
[3] Institut Pasteur, Mouse Genetics Engineering Platform, Université Paris Cité, Paris, France

Human immune system (HIS) mice provide a model to study human immune responses in vivo. Currently available HIS mouse models may harbor mouse Fc Receptor (FcR)-expressing cells that exert potent effector functions following administration of human Ig. Previous studies showed that the ablation of the murine FcR gamma chain (FcR-γ) results in loss of antibody-dependent cellular cytotoxicity and antibody-dependent cellular phagocytosis in vivo. We created a new FcR-γ-deficient HIS mouse model to compare host (mouse) versus graft (human) effects underlying antibody-mediated immune responses in vivo. FcR-γ-deficient HIS recipients lack expression and function of mouse activating FcRs and can be stably and robustly reconstituted with human immune cells. By screening blood B-cell depletion by rituximab Ig variants, we found that human FcγRs-mediated IgG1 effects, whereas mouse activating FcγRs were dominant in IgG4 effects. Complement played a role as an IgG1 variant (IgG1 K322A) lacking complement binding activity was largely ineffective. Finally, we provide evidence that FcγRIIIA on human NK cells could mediate complement-independent B-cell depletion by IgG1 K322A. We anticipate that our FcR-γ-deficient HIS model will help clarify mechanisms of action of exogenous administered human antibodies in vivo.

Keywords: ADCC · NK cells · Antibody-mediated immune responses · Fc receptors · Human immune system (HIS) mice

Additional supporting information may be found online in the Supporting Information section at the end of the article.

Correspondence: Prof. James P. Di Santo
e-mail: james.di-santo@pasteur.fr

[*]These author contributed equally to this work.

Introduction

Robust and relevant preclinical animal models remain essential tools to evaluate in vivo biological activities, pharmacodynamics as well as safety and efficacy of novel therapeutics for human disease. In this respect, human immune system (HIS) mice based on immunodeficient hosts (e.g., NOD/LtSz-*scid Il2rg*^{null} (NSG), NOD/Shi-*scid Il2rg*^{null} (NOG), and Balb/c *Rag2*^{null}*Il2rg*^{null} *Sirpa*^{NOD} (BRGS) mice) have demonstrated their value for the study of candidate vaccines, treatments for viral infections like EBV or HIV and for novel cancer therapies [1–3]. HIS mice harbor human innate and adaptive immune cells after engraftment and differentiation of human hematopoietic stem cells that generate functional cellular and humoral immune responses [4–6] and can thus be used for preclinical testing of novel therapeutic strategies, while closely mirroring the situation in humans.

Monoclonal antibodies (mAbs) represent one category of therapeutic agents that have revolutionized disease treatment, in particular those involving viral infections and cancer; this is an extremely active area of research with >100 mAbs already approved for clinical use [7]. Antibodies function by modulating immune responses through several distinct modes of action that include blocking of receptor–ligand interactions, mimicking the binding of natural ligands, direct induction of apoptosis, and mediating interactions with immune system components [8–11]. In the latter, engagement of antibodies with the complement system leads to complement-dependent cytotoxicity (CDC) [12] or complement-dependent phagocytosis (CDP) [13], whereas engagement with Fc Receptor-expressing (FcR$^+$) immune cells, such as natural killer (NK) cells, neutrophils, and macrophages, provokes antibody-dependent cellular cytotoxicity (ADCC) or antibody-dependent cellular phagocytosis (ADCP) through activation pathways involving the FcR-γ chain (encoded by *Fcer1g*) [14].

Therapeutic mAbs (Tx mAbs) are developed with human IgG isotypes (mostly IgG1, IgG4), which have differential binding to human (FcγR$^+$) hematopoietic cells and abilities to activate complement [15, 16]. The analysis of these human mAbs in preclinical HIS models is further complicated as recipients harbor functional macrophages and neutrophils [17] and may retain a functional complement system [18], which can confound the interpretation of exogenously administered Tx mAbs [19, 20]. Previous studies have shown that human IgG-based mAbs bind to mouse FcR-γ$^+$ cells in vivo [21, 22].

To define the roles for human FcR-γ$^+$ hematopoietic cells during Tx mAb administration in vivo more clearly, HIS mouse models have been developed where the contribution of activating mouse FcRs can be excluded. One approach made use of mAbs with Fc regions that have reduced or abolished binding to mouse FcRs [14, 21]. Still, these variant mAbs also show reduced or abolished human FcR binding so their ability to discriminate mouse versus human FcR activation was limited. HIS mouse models with the ablation of *Fcer1g* (lacking expression of IgG activating receptors FcγRI, FcγRIII, FcγRIV, and IgE receptor FcεRI) and *Fcgr2b* (lacking inhibitory receptor FcγRIIB) genes have been reported [23, 24]. These models provide "cleaner" systems to assess Tx mAbs activities that interact with human FcR$^+$ cells. Interestingly, hCD20$^+$ tumor cell depletion was observed in one *Fcer1g*-deficient model [24] after rituximab administration even in the absence of human immune cells suggesting additional host effector mechanisms.

In this study, we generated a novel *Fcer1g*-deficient strain using a CRIPSR/Cas9 approach in BRGS-HLA-A2^{tg}-HLA-DR2^{tg} (BRGSA2DR2; [2]) that functionally ablates mouse activating FcRs (FcγRI, FcγRIII, FcγRIV) which can bind human Ig [14, 25, 26]. We further characterized HIS mice produced in BRGSA2DR2 *Fcer1g*$^{-/-}$ recipients to identify the role of human FcR-γ$^+$ cells and other mechanisms contributing to exogenous Tx mAbs responses in vivo.

Results

Generation and validation of BRGSA2DR2 Fcer1g$^{-/-}$ mice

BRGSA2DR2 mice [2] were rendered *Fcer1g*-deficient using CRISPR/Cas9-mediated gene targeting (see "Materials and methods" section). Genomic DNA sequencing revealed a 66-bp Exon 2 deletion (Supporting Information Fig. 1A and C) resulting in Exon 2 skipping upon transcription (Supporting Information Fig. 1B and C). In silico mRNA sequence analysis predicted a frameshift truncated protein of 27 amino acids (Supporting Information Fig. 1D and E).

Fcer1g gene deletion impairs the expression of murine CD16/CD32 (FcγRIII/FcγRII), CD64 (FcγRI), and the IgE receptor (FcεRI) [25]. We observed no significant difference in CD16/CD32 expression in Gr-1$^+$ neutrophils between *Fcer1g* wt and heterozygous BRGSA2DR2 mice, whereas CD16/CD32 expression in *Fcer1g*$^{-/-}$ mice was significantly reduced (Fig. 1A) confirming previous observations that residual FcRa chain expression is *Fcer1g*-independent [25]. In contrast, CD64 and FcεRI staining was abrogated in CD11b$^+$ and CD11b$^-$ cells, respectively (Fig. 1B and C; Supporting Information Fig. 2A) consistent with previous reports [25]. Absence of mouse FcR-γ chain protein in spleen cells was confirmed by intracellular staining (Supporting Information Fig. 2B). We performed an IgG-dependent passive systemic anaphylaxis assay (Fig. 1D) to assess FcγRIII function [27]. A significant drop in body temperature consistent with acute anaphylaxis was seen in *Fcer1g* wt and heterozygous mice, whereas *Fcer1g*-deficient mice maintained stable body temperature over time (Fig. 1E). Together, these results demonstrate successful inactivation of the FcR-γ chain in BRGSA2DR2 mice at DNA, mRNA, protein, and functional levels.

Efficient human immune cell engraftment in BRGSA2DR2 Fcer1g$^{-/-}$ mice

We assessed human cell reconstitution [2] after CD34$^+$ hematopoietic stem cell engraftment in this new BRGSA2DR2

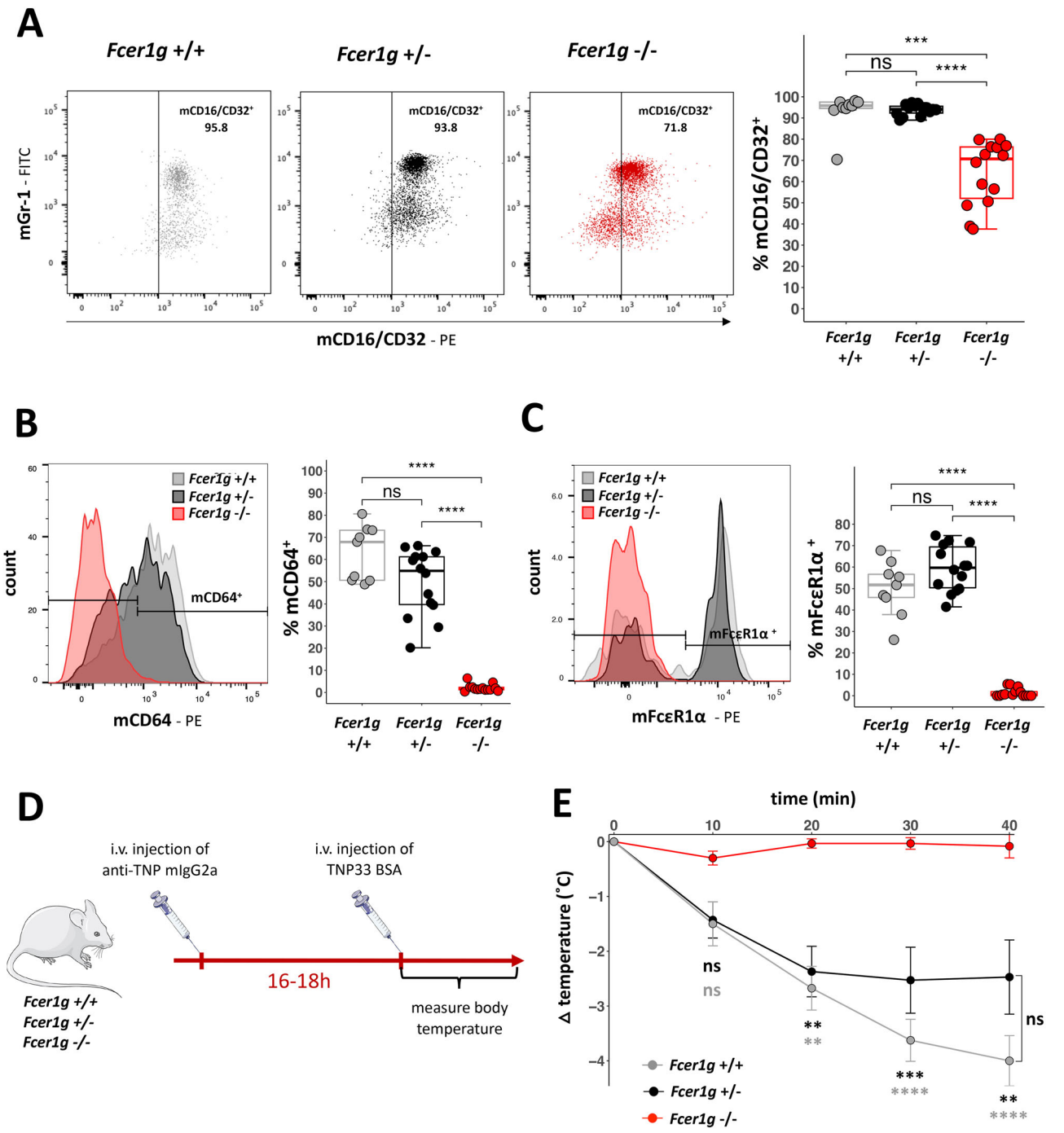

Figure 1. Validation of Fcer1g-deficient BRGSA2DR2 hosts. (A–C) Representative FACS staining in blood (left) and quantification of frequency of positive cells (right) in *Fcer1g* wt (gray; n = 9), *Fcer1g*$^{+/-}$ (black; n = 14), *Fcer1g*$^{-/-}$ (red; n = 14) BRGSA2DR2 mice for (A) mCD16/32 in monocytes (CD11b^{+}, SCC-A^{low}, mGr-1$^{low/mid}$), (B) mCD64 in macrophages (CD11b^{+}, SSC-A^{lo}, Gr1$^{mid/-}$), and (C) mFcεR-1α in CD11b-, Gr1-cells, respectively; each dot represents one mouse, and data include results from three independent experiments. Group means were compared by Kruskal–Wallis test. (D) Schematic diagram of passive systemic anaphylaxis (PSA) assay. (E) Body temperature difference $\Delta T = (T_{x\min} - T_{0\min})$ in °C over time in PSA assay after TNP_{33}-BSA mIgG2a injection in *Fcer1g* wt (gray; n = 4), *Fcer1g*$^{+/-}$ (black; n = 7), *Fcer1g*$^{-/-}$ (red; n = 6) BRGSA2DR2 mice. Means between groups were compared by Tukey's HSD test at each timepoint; statistical significance is indicated (ns: not significant). Data are represented as mean ± SEM and representative of two independent experiments.

strain. Human immune cell subset composition in the blood at 12 weeks postgraft and in the organs at 16 weeks postgraft was similar when comparing BRGSA2DR2 *Fcer1g* WT or heterozygous HIS mice (referred to as "HIS") with BRGSA2DR2 *Fcer1g*-deficient HIS mice (referred to as "HIS *Fcer1g*$^{-/-}$"). There were no significant differences in the degree of humanization in the blood or in different organs in the absence of *Fcer1g* (Supporting Information Fig. 3A and C). No significant differences in percentages or absolute numbers of total hCD45 (Fig. 2A and D), CD19$^+$ B cells (Fig. 2B and E), CD3$^+$ T cells (Fig. 2C and F), NKp46$^+$CD94$^+$ NK cells (Fig. 2G), CD4$^+$ or CD8$^+$ T cells (Fig. 2H and I), or ratio of CD4/CD8 T cells (Supporting Information Fig. 3B) were observed in the blood, spleen, BM, and liver between HIS and HIS *Fcer1g*$^{-/-}$ mice, indicating comparable human immune cell differentiation in this novel *Fcer1g*-deficient HIS mouse model to previously reports [4–6, 17, 24, 28].

OKT8-mediated depletion of hCD8a$^+$ cells in HIS mice requires Fcer1g

We next assessed exogenous antibody-mediated depletion in HIS *Fcer1g*$^{-/-}$ mice. The anti-hCD8a antibody (OKT8) has been demonstrated to efficiently deplete human CD8a$^+$ T cells in several HIS mouse models [28, 29]. This mIgG2a antibody binds murine FcγRs and can activate complement via C1q binding [22, 30]. OKT8 injection into HIS mice efficiently depleted hCD8a$^+$ T cells in the blood, whereas only partial depletion was seen in HIS *Fcer1g*$^{-/-}$ mice (Supporting Information Fig. 4A and B), demonstrating the involvement of mouse *Fcer1g*-dependent as well as *Fcer1g*-independent mechanisms. We could exclude OKT8-mediated inhibition (masking) as an explanation for the observed hCD8a$^+$ T-cell loss as hCD8b (which forms heterodimers with the hCD8 alpha chain [31] and is co-expressed on most hCD8a$^+$ T cells in our HIS mice) expression was similarly decreased (Supporting Information Fig. 4A and C). Frequencies of hCD19$^+$ B cells (Supporting Information Fig. 4D) were unaffected, confirming specificity of the OKT8-mediated depletion.

Deciphering mechanisms that contribute to Ig-mediated cell depletion in HIS mice

We next dissected the human FcR-dependent mechanisms underlying exogenous antibody-mediated depletion in HIS mice. For this, we studied depletion of human B cells following administration of the Tx anti-hCD20 mAb Rituximab (Fig. 3A). One advantage of this model is the availability of human IgG variants with different isotypes and capacities to bind and activate complement [15, 16, 23, 32]. In a similar fashion to the method described in Lux *et al.* [23], we analyzed hCD19$^+$ cells before and after rituximab injection as hCD19 is co-expressed on the majority of hCD20$^+$ B cells in the HIS mice (Supporting Information Fig. 5A).

We first compared depletion mediated by hIgG1 and hIgG4 variants, the latter displaying limited affinity for human FcRs (except for CD64), while retaining strong binding to mouse FcRs and weakly activating complement [16, 22, 33–38]. The hIgG1 Rituximab variant similarly reduced human B cells in both HIS and HIS *Fcer1g*$^{-/-}$ mice (Fig. 3B and C) suggesting the involvement of human FcR$^+$ effector cells and/or mouse complement in the depletion. In contrast, the hIgG4 Rituximab variant, while able to deplete human B cells in HIS mice, was significantly less efficient in HIS *Fcer1g*$^{-/-}$ mice (Fig. 3B and C) confirming earlier studies [23]. These results demonstrate that hIgG4 mAbs can deplete target cells in HIS mouse models, and this largely occurs through activating FcR$^+$ mouse cells. Interestingly, partial hIgG4 antibody-mediated depletion still occurred in HIS *Fcer1g*$^{-/-}$ mice (compared to control PBS injected mice; Fig. 3C) revealing a non-FcR-γ-dependent mechanism that could include mouse complement.

In order to delineate effects mediated by Rituximab in HIS *Fcer1g*$^{-/-}$ mice via human FcR$^+$ cells from those involving complement, we analyzed the depletion capacity of a Rituximab variant (IgG1_K$_{322}$A) that fails to bind complement or induce CDC and has reduced binding to human FcγRIIA and FcγRIIIA with a roughly twofold reduction in ADCC compared to IgG1 [39]. Human B-cell depletion by the Rituximab IgG1_KA variant was clearly reduced in HIS *Fcer1g*$^{-/-}$ mice compared to Rituximab IgG1 control mAb (Fig. 3B and C). These results indicate that complement-dependent mAb depletion operates in HIS mice in the absence of activating mouse FcRs.

In most Rituximab IgG1_KA-injected HIS *Fcer1g*$^{-/-}$ mice, little or no human B-cell depletion was detected. Nevertheless, IgG1_KA-injected HIS *Fcer1g*$^{-/-}$ mice had significantly higher depletion compared with PBS-injected HIS *Fcer1g*$^{-/-}$ control mice (Fig. 3C) suggesting the involvement of human FcR$^+$ cells. We verified the specificity of Rituximab treatment and found no significant differences in CD8$^+$ T-cell numbers in HIS and HIS *Fcer1g*$^{-/-}$ mice injected with Rituximab IgG1 or IgG1_KA versus controls (Supporting Information Fig. 5C). We noticed that the degree of depletion in Rituximab IgG1_KA-injected HIS *Fcer1g*$^{-/-}$ mice strongly correlated with the percentage of human NK cells present in the blood of individual HIS mice (Fig. 3D). We failed to find a similar correlation with other human immune cell subsets, for example, CD8$^+$ T cells (Supporting Information Fig. 5D).

To further test the potential role for human NK cells, we expanded these FcγR$^+$ effector cells in HIS *Fcer1g*$^{-/-}$ mice using exogenous IL-15. Previous work from our laboratory [40] showed that human IL-15 supplementation in HIS mice increases NK cell effector functions and human CD16 expression. We observed significantly higher levels of hCD19 B-cell depletion in IL-15 boosted compared with control Rituximab IgG1_KA-treated HIS *Fcer1g*$^{-/-}$ mice (Fig. 3C). Furthermore, human B-cell depletion correlated strongly with enhanced CD16 expression on human NK cells in IL-15 boosted HIS mice (Fig. 3E), whereas FcR$^+$ human macrophages were not affected by the IL-15 boost (Supporting Information Fig. 5E). These results suggest that an inducible ADCC activity by human NK cells underlies the human B-cell depletion in rituximab IgG1_KA-treated HIS *Fcer1g*$^{-/-}$ mice.

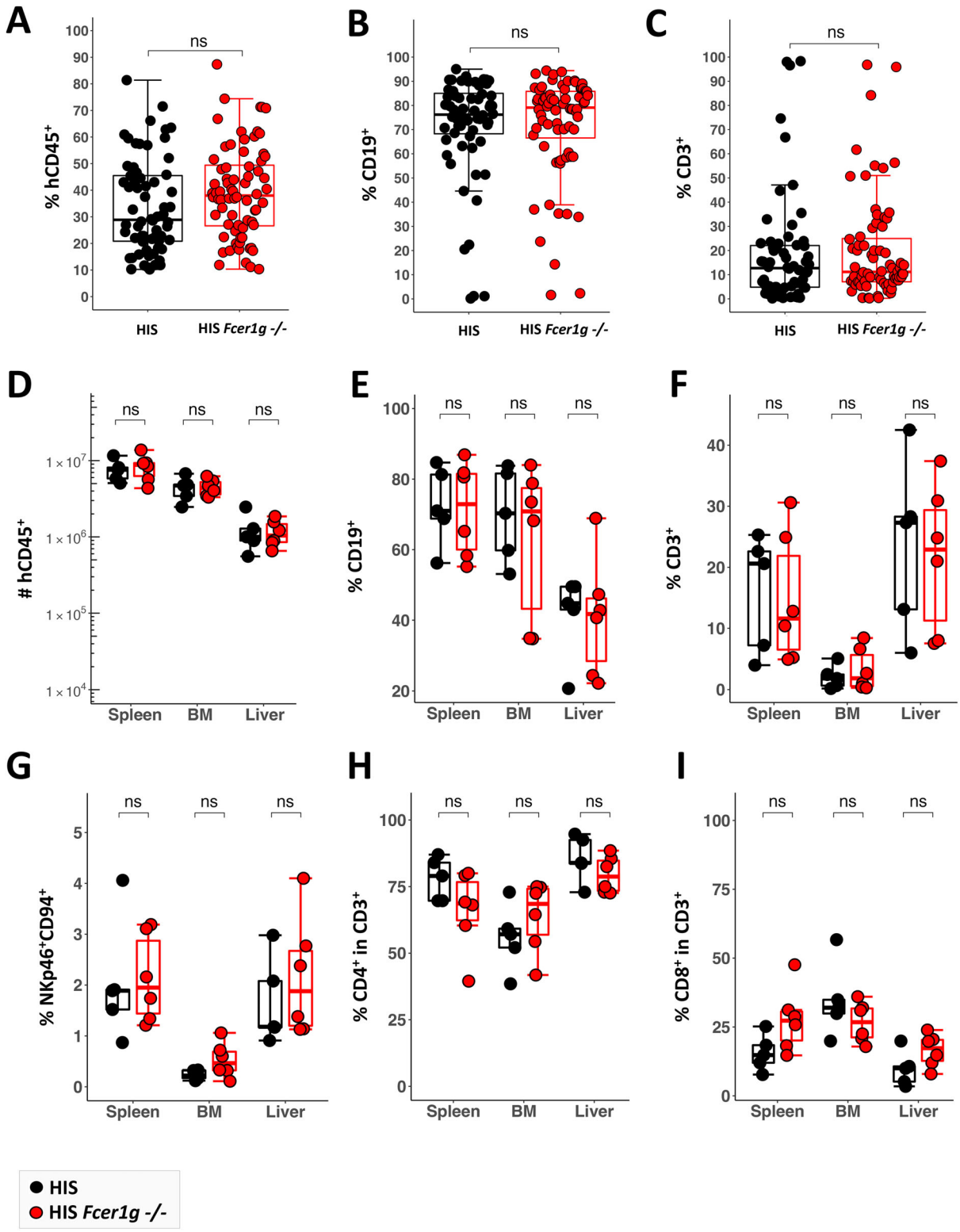

Figure 2. Human immune cell reconstitution in BRGSA2DR2 *Fcer1g*$^{-/-}$ mice. Quantification of human immune cell populations in human immune system (HIS) *Fcer1g* wt mice (black) versus HIS *Fcer1g*$^{-/-}$ mice (red). (A–C) In blood at 12 weeks postgrafting (wpg), (A) percentage of hCD45 calculated as %hCD45 cells = 100*hCD45/(hCD45 + mCD45), (B) frequency of CD19^{+} B cells in hCD45 cells, and (C) frequency of CD3^{+} T cells in hCD45 cells. (D–I) For the spleen, BM and liver at 16 wpg. (D) Absolute numbers of hCD45 per organ (for BM for one femur and one tibia). Frequency of (E) CD19^{+} B cells, (F) CD3^{+} T cells, (G) NKp46^{+} and CD94^{+} NK cells in hCD45 and (H) CD4^{+} and (I) CD8^{+} in total CD3^{+} T cells. Each dot represents one mouse, and data from the blood are representative for 21 mice (>6 independent experiments) and from the organs for 2 independent experiments. Pairwise comparison in the blood was done by Wilcoxon test, and Kruskal–Wallis test was used for multiple comparisons of means in the organs.

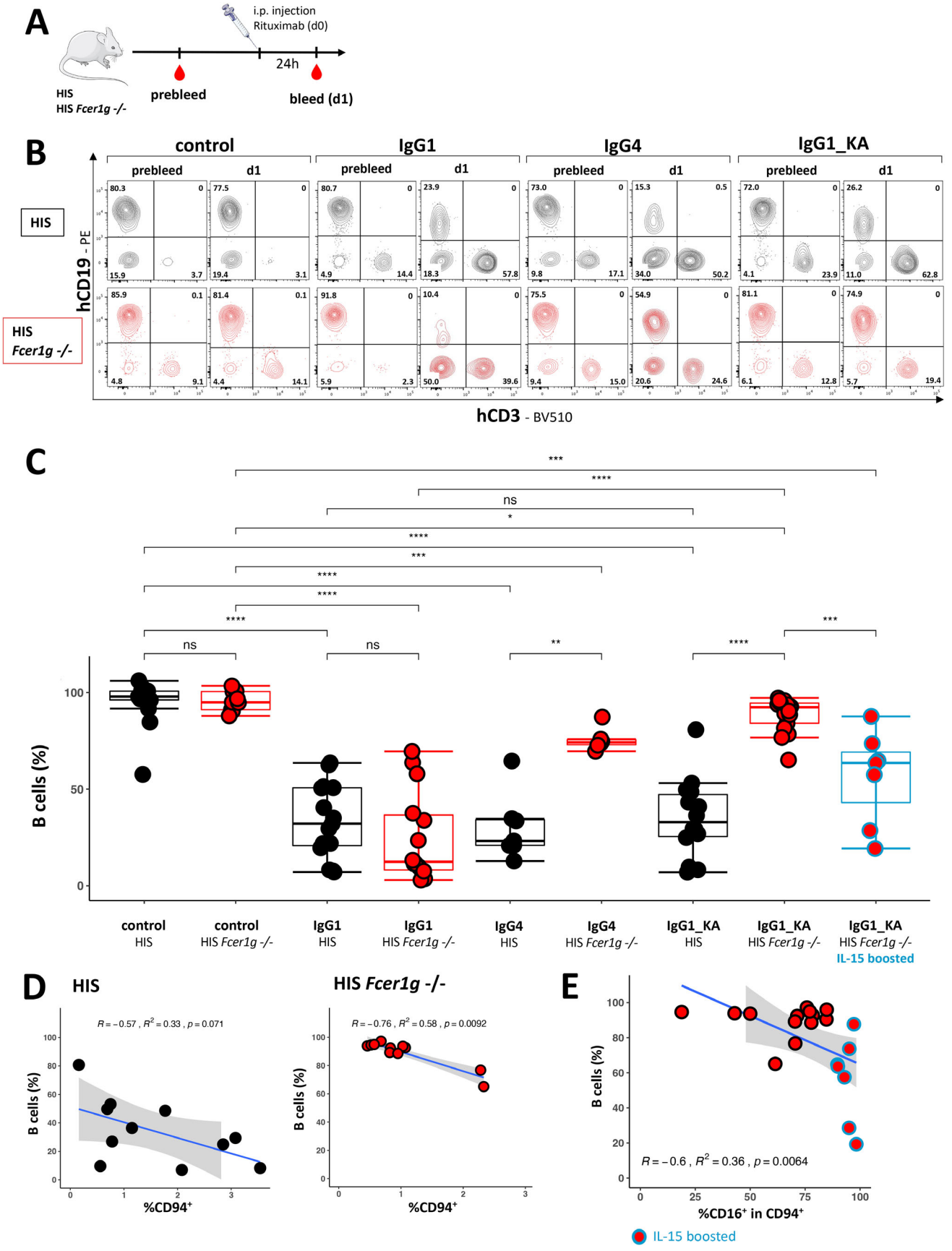

Discussion

Antibodies elicit diverse effects during immune responses as soluble Ig, complexed with antigens (immune complexes) or bound to relevant targets on the cell surface. Subsequent steps may involve the activation of effector cells (via FcRs) or complement, leading to ADCC, ADCP, complement-dependent phagocytosis, or CDC [12–14, 41, 42]. As many current HIS mouse models may possess endogenous mouse FcR-bearing hematopoietic cells and may retain a functional complement system [18, 43], interpretation of effects elicited by Tx mAbs in reconstituted HIS mice is challenging [19, 20]. Recently, several FcR-γ-deficient HIS mouse models based on NOG, NSG, or *Rag2*$^{-/-}$*/Il2rg*$^{-/-}$ backgrounds were reported [23, 24, 44, 45]. Here we describe a FcR-γ-deficient BRGSA2DR2 strain that can be robustly reconstituted to generate HLA-educated HISs. Together, these new models have provided important insights into specific roles for mouse and human FcR-γ^{+} cells as well as complement in HIS mice receiving exogenous Tx mAbs.

One consistent finding observed in these different FcR-γ-deficient HIS models is the important role played by residual mouse FcR^{+} cells in mediating effects of Tx mAbs. This was first shown in immunocompetent and immunodeficient mouse models [43–46] and subsequently in HIS mice [23, 24, 47, 48] in the context of tumor rejection. The differential effects mediated by hIgG1 and hIgG4 isotypes in HIS mice were initially revealed in FcR-γ-deficient HIS mice using human B cell or mouse platelet-depleting antibodies [23, 47]; results we confirm here using B-cell-depleting Rituximab. Katano *et al.* showed the important role for mouse FcR (most likely involving activating forms) in human tumor rejection using an NOG-based model [24], confirming earlier work [43, 45, 46]. Still the murine effector cells responsible for the biological effects varied in these reports, including circulating neutrophils and/or tissue macrophages.

Here we extend the list of potential host mechanisms responsible for Tx mAb effects in HIS mice to include mouse complement. We used an Fc mutant of Rituximab IgG1, which harbors the $K_{322}A$ point mutation that abolishes C1q binding [39]. B-cell depletion was less efficient using the KA variant Rituximab in HIS *Fcer1g*$^{-/-}$ mice, suggesting an important contribution of complement to cell depletion in our HIS mouse model. Still, a twofold reduction in ADCC and binding of IgG1_KA via FcγRIIA and FcγRIIIA to human immune cells has been reported [39] suggesting that lower ADCC/ADCP mediated by human FcγR^{+} cells may also be involved.

FcR-γ-deficient HIS mice may be useful in defining the contribution of human FcγR^{+} cells to effects mediated by exogenously delivered Tx mAbs or other immunomodulators that can bind FcRs (e.g., Fc-fusion proteins [49]). Katano *et al.* [48] used an adoptive cell transfer model in IL-15Tg FcR-γ-deficient NOG mice to suggest that human NK cells could be involved in the elimination of human tumor xenografts, although the precise mechanism remained unclear. Here, we showed in fully reconstituted FcR-γ-deficient BRGSA2DR2 HIS mice that NK cells were important effectors of rituximab and that boosting human CD16^{+} NK cells (via exogenous IL-15) could amplify B-cell depletion elicited by the IgG1_KA rituximab variant. To our knowledge, this result represents the first direct demonstration of in vivo ADCC mediated by human NK cells.

Neutrophils, dendritic cells (DCs) and macrophages are the other main human FcR^{+} hematopoietic cells that develop in HIS mice and may also be involved in antibody-dependent effects. As such, use of BRGSA2DR2 *Fcer1g*$^{-/-}$ HIS mice carrying an Flk2Flt3 mutation, which develop enhanced human DCs and innate lymphoid cells after hFlt3L administration [17, 50], may help clarify the role for human FcR^{+} DCs in mediating Tx mAbs effects in HIS mice. Identification of the precise human FcγR^{+} cell subsets involved in antibody-mediated cellular effects in vivo will allow better characterization of the properties of Tx mAbs to tailor them to be most efficient in diverse disease settings.

Study limitation and future perspectives

The effect of antibody depletion on blood cells in HIS mice was performed in order to have an accurate pretreatment control. Future studies should examine the extent of depletion in HIS organs such as the spleen and BM to confirm the observations made in this work.

Materials and methods

Ethics statement

Animals were housed in ventilated cages under specific-pathogen-free conditions with humane care. Experiments were approved by the Institut Pasteur Ethics Committee (#2013-0131, dap210088), authorized by the French Ministry of Education and Research (#02162.02, APAFIS # 35066–2022013116538847v2), and conducted in compliance with French and European regulations.

Figure 3. Human B-cell depletion in human immune system (HIS) mice by rituximab variants. (A) Scheme of hCD20 depletion by rituximab injection. (B) Representative FACS plots of blood from HIS (top) and HIS *Fcer1g*$^{-/-}$ (bottom) mice at prebleed or at d1 (24 h after injection) for each antibody variant. (C) B cells (%) = %CD19 (d1)/%CD19 × 100 (prebleed) in HIS (black), HIS *Fcer1g*$^{-/-}$ (red), and IL-15 boosted HIS *Fcer1g*$^{-/-}$ (red; blue outline) mice injected with either NaCl (control) or variants of rituximab with human IgG1, IgG4, or IgG1_KA Fc fragment. Kruskal–Wallis test was used for multiple comparisons of means between groups. (D) Spearman correlation analysis of B cells (%)with %CD94^{+} NK cells in hCD45 at prebleed for rituximab IgG1_KA injected HIS (left) and HIS *Fcer1g*$^{-/-}$ (right) mice. (E) The Spearman correlation analysis of B cells (%) with %CD16^{+} NK cells (CD19^{-}, CD3^{-}, CD94^{+}) in hCD45 at prebleed for rituximab IgG1_KA injected HIS *Fcer1g*$^{-/-}$ mice with or without IL-15 boost. Each dot represents one mouse, and data include results from two independent experiments for all conditions.

Mice and generation of BRGSFA2DR2 Fcer1g-deficient strain

BRGSF (BALB/c *Rag2*^{tm1Fwa} *Il2rg*^{tm1Cgn} *Sirpa*^{NOD} *Flt3*^{tm1lrl}) and BRGSA2DR2 (Balb/c *Rag2*$^{-/-}$ *Il2rg*$^{-/-}$ *Sirpa*^{NOD} Tg(HLA-A/H2-D/B2M)^{1Bpe}, Tg(HLA-DRB1*1501)$^{\#Lfug}$) have been previously described [2, 50]. BRGSFA2DR2 mice were generated and used as hosts for CRISPR-mediated modification of the *Fcer1g* locus (Mouse Genetics Engineering Center of Institut Pasteur). The following guide sequences were chosen by using the CRISPOR Web tool (https://crispor.tefor.net/) [51], and guide 1: TGA GTC GAC AGT AGA GTA GG and guide 2: TCC AGG ATA TAG CAG AGC TG targeting exon 2 of the *Fcer1g* gene were each cloned into a PX330 expression vector (a gift from F. Zhang, the Broad Institute of Massachusetts Institute of Technology and Harvard University, Cambridge, MA; plasmid 42230; Addgene [52]). To generate m *Fcer1g* gene, zygotes were microinjected with pX330 as previously described [53].

PCR and sequencing

Extraction of genomic DNA from biopsies using proteinase K (Eurobio) at 56°C and DNA was subsequently precipitated with ethanol. mRNA was extracted from blood with the QIAamp RNA Blood Mini Kit (Qiagen). Retro transcription of mRNA into cDNA was done using SuperScript III Reverse Transcriptase (Invitrogen) with Random Hexamers (Invitrogen). DNA or cDNA spanning the Fcer1g Exon 2 was amplified by PCR; primers for genomic DNA, forward (Fwd): 5′-TTT TCC CTT CAG ACC ATG GGG-3′, reverse (Rev): 5′-CCC ATG GGC ACC CTG TAT C-3′; for cDNA, Fwd: 5′-CAG CTG CGC AGT TCT GTC A-3′, Rev: 5′-ATC TGC TTT CTC ACG GCT GG-3′. For sequencing, the PCR product was run on an agarose gel, the respective bands were cut out, and the DNA was purified with the NucleoSpin Gel and PCR clean-up kit (Macherey-Nagel) before sequencing (Eurofins Genomics, Cologne). Analysis, primer design, and protein prediction used public data sources (https://www.ncbi.nlm.nih.gov).

Passive systemic anaphylaxis assay (PSA)

Mice between 9 and 15 weeks old were sensitized by intravenous (i.v.) injection of 200 μg mIgG2a-anti-trinitrophenyl (TNP) (clone Hy-1.2) per mouse. After 24 h, they were i.v. injected with 100 μg BSA substituted with 33 molecules of TNP (TNP_{33}-BSA)/mouse, and the body temperature was measured via a rectal thermometer before injection (t0) and at 10, 20, 30, and 40 min after injection [27].

Tissue/organ processing and cell isolation

To obtain single cell suspensions, spleens were dissociated using 40 μm cell strainers (Falcon). To extract BM cells, one femur and one tibia were crushed with a mortar and pestle, and cells were filtered with a 100 μm cell strainer (Falcon). Red blood cells were lysed using ACK buffer (NH_4Cl, $KHCO_3$, EDTA in H_2O; pH 7.3). The liver was cut into small pieces, digested at 37°C with 25 μg/mL Liberase TL (Roche) and 100 μg/mL DNase I (Roche), passed through a 100 μm cell strainer and mononuclear cells isolated by Percoll (GE Healthcare) density gradient centrifugation. All cell suspensions were filtered through cell-strainer caps (Falcon) before counting with Trypan blue (Life Technologies) and staining for flow cytometry. For all organ processing steps, RPMI Medium 1640 (Life Technologies) with 5% fetal calf serum (Eurobio) was used.

Flow cytometry

Flow cytometric analysis was performed in accordance with published guidelines [54]. Whole blood collected in EDTA-coated Microvettes (Sarstedt) was directly stained with fluorochrome-conjugated antibodies (Table 1) at 4°C for 30 min, erythrocytes were lysed, and samples fixed with FACS Lysing solution (BD). For the organ-derived cells, a maximum of 2×10^6 cells were used for analysis, prior to staining they were incubated for 10 min at RT with IgG from human serum (Sigma-Aldrich) and FcR blocking reagent Mouse (Miltenyi). For surface marker staining, respective fluorochrome-conjugated antibodies (Table 1), for dead cell exclusion Viability dye eFluor 506 (Invitrogen) and cell number determination CountBright absolute counting beads (Invitrogen), were diluted in brilliant stain buffer (BD). Staining was done at 4°C for 30 min, after washing cells were fixed in 4% PFA (EMS) and resuspended for acquisition. Washing steps were done in FACS buffer (1× DPBS (Gibco) with 2% fetal calf serum (eurobio), 2 mM EDTA (Invitrogen)). For intra cellular staining cells were fixed by Cytofix/Cytoperm (BD) and subsequently incubated with intra cellular antibody diluted in Perm/Wash (BD) for 30 min at 4°C. Data were acquired on an LSR Fortessa (BD) and analyzed with FlowJo 10 software (FlowJo LLC).

Generation of human immune system (HIS) mice

HIS mice were generated in BRGSA2DR2 *FceR1g*$^{+/-}$ and *FceR1g*$^{-/-}$ mice as previously described [2, 17, 50, 55]. Briefly, human fetal liver (Advanced Bioscience Resources Inc.) CD34$^+$ cells were isolated using MicroBead Kits (Miltenyi). CD34, CD38, and HLA-A2 expressions were phenotyped by FACS and the HLA class II allele haplotype analysis by PCR (LABType SSO, One Lambda). 7–15 × 10 [4] CD34$^+$CD38$^-$ cells from HLA-A*02$^+$ HLA-DRB1*15$^+$ donors, or from 1:1 mixtures of HLA-A*02$^+$ and HLA-DRB1*15$^+$ donors, were intrahepatically injected into 2–10-day-old mice that had been sublethally irradiated (3 Gy). The efficiency of humanization in the blood was assessed by flow cytometry using the following formula: %hCD45 × 100/(%hCD45 + %mCD45); only mice with humanization ≥10% were used for experiments.

Table 1. List of antibodies used in this study.

Antigen	Fluorochrome	Clone	Reactivity	Supplier	Catalog number
CD3	BV510	SK7	Human	BioLegend	344828
CD3	APC-Vio770	REA613	Human	Miltenyi Biotec	130-113-136
CD4	APC	RPA-T4	Human	BD	555349
CD4	BUV496	SK3	Human	BD	612936
CD11b	AF700	M1/70	Mouse/human	eBioscience	56-0112-82
CD16	BUV737	3G8	Human	BD	564434
CD16	BUV805	3G8	Human	BD	748850
CD16/CD32	PE	2.4G2	Mouse	BD	561727
CD19	PE	HIB19	Human	BioLegend	302208
CD19	PE-CF594	HIB19	Human	BD	562294
CD20	BV786	2H7	Human	BioLegend	302356
CD45	APC-Cy7	30-F11	Mouse	BD	557659
CD45	PerCP-Cy5.5	HI30	Human	BD	564105
CD45	FITC	30-F11	Mouse	BioLegend	103108
CD45	BUV395	HI30	Human	BD	563792
CD45	BV650	30-F11	Mouse	BD	563410
CD45	BUV805	HI30	Human	BD	612891
CD64	PE	X54-5/7.1	Mouse	BD	558455
CD8a	PE-CF594	RPA-T8	Human	BD	562282
CD8a	BV786	RPA-T8	Human	BioLegend	301046
CD8b	PE-Cy7	SIDI8BEE	Human	eBioscience	25-5273-42
CD94	FITC	DX22	Human	BioLegend	305504
CD94	PerCP-Vio700	REA113	Human	Miltenyi Biotec	130-119-763
FCER1A	PE	MAR-1	Mouse	eBioscience	12-5898-82
FCER1G	FITC		Human/mouse	Merck-Millipore	FCABS400F
Gr-1	FITC	RB6-8C5	Mouse	BD	553127
NKp46	BV421	9E2/NKp46	Human	BD	564065

Antibody-mediated depletion of human cell subsets in vivo

For $CD8a^+$ cell depletion, HIS mice were prebled 3 days before i.p. (intraperitoneal) injection with 100 μg/mouse of antihuman CD8a antibody OKT8 (BioXcell) in PBS, and control mice were injected with only PBS and bled at day 4 (d4) postinjection. For $CD20^+$ cell depletion, HIS mice were prebled 6 days before i.p. injection with 25 μg/mouse of antihuman CD20 antibody rituximab in the IgG1, $IgG4_{S228P}$, and $IgG1\_K_{322}A$ format or saline solution and bled at day 1 (d1) postinjection. Tx Abs are generally used in the stabilized $IgG4_{S228P}$ format to prevent Fab arm exchange of IgG4 hemi-molecules [56].

Human IL15 boost in vivo

HIS mice were injected four times i.p. with 100 μL of hIL-15Ra-Fc (7.5 μg) + hIL-15 (2.5 μg) (R&D Systems) every 3–4 days; 1 day after the last injection mice were prebled, injected with IgG1_KA, and bled at d1 postantibody injection.

Statistical analysis

Data were compared with unpaired nonparametric tests as indicated in the figure legends, and correlations were tested by the Spearman correlation using RStudio (Version 1.4.1106). p Values are indicated as ns: $p > 0.05$, $*p \leq 0.05$, $**p \leq 0.01$, $***p \leq 0.001$, $****p \leq 0.0001$.

Acknowledgments: We thank the Center for Translational Science Cytometry and Biomarkers Unit of Technology and Service and the Central Animal Facility at Institut Pasteur. We thank P. Bousso (Institut Pasteur) for providing FcR-γ-deficient B6 mice. JPD receives financial support from the Institut Pasteur, the Institut National de la Santé et de la Recherche Médicale (INSERM), and the Vaccine Research Institute (to GG-Z). The work was supported in part by grants from the European Union's Horizon 2020 research and innovation program under grant agreement no.

847939, and from the ANRS-MIE Agence Nationale de Recherches sur le Sida et les Hépatites Virales/Maladies Infectieuses Emergentes (grant ECTZ91652) (to HS-M). PB acknowledges funding from the French National Research Agency grants ANR-18-CE15-0001 project Autoimmuni-B, from the Institut Carnot Pasteur Microbes et Santé, from the Institut Pasteur and from the Institut National de la Santé et de la Recherche Médicale (INSERM). FJ is employed by the Centre National de la Recherche Scientifique (CNRS). AT received funding from the European Union's Horizon 2020 research and innovation program under the Marie Skłodowska-Curie (Grant Agreement No. 765104).

Conflict of interest: The authors declare no commercial or financial conflict of interest.

Data availability statement: The data that support the findings of this study are available from the corresponding author upon reasonable request.

Peer review: The peer review history for this article is available at https://publons.com/publon/10.1002/eji.202350454.

References

1 **van Zyl, D. G., Tsai, M.-H., Shumilov, A., Schneidt, V., Poirey, R., Schlehe, B., Fluhr, H. et al.**, Immunogenic particles with a broad antigenic spectrum stimulate cytolytic T cells and offer increased protection against EBV infection ex vivo and in mice. *PLoS Pathog.* 2018. **14**: e1007464.

2 **Masse-Ranson, G., Dusséaux, M., Fiquet, O., Darche, S., Boussand, M., Li, Y., Lopez-Lastra, S. et al.**, Accelerated thymopoiesis and improved T-cell responses in HLA-A2/-DR2 transgenic BRGS-based human immune system mice. *Eur. J. Immunol.* 2019. **49**: 954–965.

3 **Capasso, A., Lang, J., Pitts, T. M., Jordan, K. R., Lieu, C. H., Davis, S. L., Diamond, J. R. et al.**, Characterization of immune responses to anti-PD-1 mono and combination immunotherapy in hematopoietic humanized mice implanted with tumor xenografts. *J. Immunother. Cancer* 2019. **7**: 37.

4 **Shultz, L. D., Lyons, B. L., Burzenski, L. M., Gott, B., Chen, X., Chaleff, S., Kotb, M. et al.**, Human LYMPHOID and myeloid cell development in NOD/LtSz-*scid IL2R* γ^{null} mice engrafted with mobilized human hemopoietic stem cells. *J. Immunol.* 2005. **174**: 6477–6489.

5 **Ito, M., Hiramatsu, H., Kobayashi, K., Suzue, K., Kawahata, M., Hioki, K., Ueyama, Y. et al.**, NOD/SCID/γcnull mouse: an excellent recipient mouse model for engraftment of human cells. *Blood* 2002. **100**: 3175–3182.

6 **Legrand, N., Huntington, N. D., Nagasawa, M., Bakker, A. Q., Schotte, R., Strick-Marchand, H., De Geus, S. J. et al.**, Functional CD47/signal regulatory protein alpha (SIRPα) interaction is required for optimal human T- and natural killer—(NK) cell homeostasis in vivo. *Proc. Natl. Acad. Sci. USA* 2011. **108**: 13224–13229.

7 **Mullard, A.**, FDA approves 100th monoclonal antibody product. *Nat. Rev. Drug Discov.* 2021. **20**: 491–495.

8 **Reinherz, E. L., Hussey, R. E. and Schlossman, S. F.**, A monoclonal antibody blocking human T cell function. *Eur. J. Immunol.* 1980. **10**: 758–762.

9 **Kaye, J., Porcelli, S., Tite, J., Jones, B. and Janeway, C. A.**, Both a monoclonal antibody and antisera specific for determinants unique to individual cloned helper T cell lines can substitute for antigen and antigen-presenting cells in the activation of T cells. *J. Exp. Med.* 1983. **158**: 836–856.

10 **Reff, M. E., Carner, K., Chambers, K. S., Chinn, P. C., Leonard, J. E., Raab, R., Newman, R. A. et al.**, Depletion of B cells in vivo by a chimeric mouse human monoclonal antibody to CD20. *Blood* 1994. **15**: 435–445.

11 **Könitzer, J. D., Sieron, A., Wacker, A. and Enenkel, B.**, Reformatting rituximab into human IgG2 and IgG4 isotypes dramatically improves apoptosis induction in vitro. *PLoS One* 2015. **10**: e0145633.

12 **Di Gaetano, N., Cittera, E., Nota, R., Vecchi, A., Grieco, V., Scanziani, E., Botto, M. et al.**, Complement activation determines the therapeutic activity of rituximab in vivo. *J. Immunol.* 2003. **171**: 1581–1587.

13 **Walbaum, S., Ambrosy, B., Schütz, P., Bachg, A. C., Horsthemke, M., Leusen, J. H. W., Mócsai, A. et al.**, Complement receptor 3 mediates both sinking phagocytosis and phagocytic cup formation via distinct mechanisms. *J. Biol. Chem.* 2021. **296**: 100256.

14 **Bruhns, P. and Jönsson, F.**, Mouse and human FcR effector functions. *Immunol. Rev.* 2015. **268**: 25–51.

15 **Yu, J., Song, Y. and Tian, W.**, How to select IgG subclasses in developing anti-tumor therapeutic antibodies. *J. Hematol. Oncol.* 2020. **13**: 45.

16 **Bruhns, P., Iannascoli, B., England, P., Mancardi, D. A., Fernandez, N., Jorieux, S. and Daëron, M.**, Specificity and affinity of human Fcγ receptors and their polymorphic variants for human IgG subclasses. *Blood* 2009. **113**: 3716–3725.

17 **Li, Y., Mention, J-J., Court, N., Masse-Ranson, G., Toubert, A., Spits, H., Legrand, N. et al.**, A novel Flt3-deficient HIS mouse model with selective enhancement of human DC development. *Eur. J. Immunol.* 2016. **46**: 1291–1299.

18 **Yamauchi, T., Takenaka, K., Urata, S., Shima, T., Kikushige, Y., Tokuyama, T., Iwamoto, C. et al.**, Polymorphic Sirpa is the genetic determinant for NOD-based mouse lines to achieve efficient human cell engraftment. *Blood* 2013. **121**: 1316–1325.

19 **Lux, A. and Nimmerjahn, F.**, Of mice and men: the need for humanized mouse models to study human IgG activity in vivo. *J. Clin. Immunol.* 2013. **33**: S4–S8.

20 **Bournazos, S., DiLillo, D. J. and Ravetch, J. V.**, Humanized mice to study FcγR function. *Curr. Top. Microbiol. Immunol.* 2014. **382**: 237–248.

21 **Overdijk, M. B., Verploegen, S., Ortiz Buijsse, A., Vink, T., Leusen, J. H. W., Bleeker, W. K. and Parren, P. W. H. I.**, Crosstalk between human IgG isotypes and murine effector cells. *J. Immunol.* 2012. **189**: 3430–3438.

22 **Wang, Yu., Krémer, V., Iannascoli, B., Goff, O. R-Le., Mancardi, D. A., Ramke, L., De Chaisemartin, L. et al.**, Specificity of mouse and human Fcgamma receptors and their polymorphic variants for IgG subclasses of different species. *Eur. J. Immunol.* 2022. **52**: 753–759.

23 **Lux, A., Seeling, M., Baerenwaldt, A., Lehmann, B., Schwab, I., Repp, R., Meidenbauer, N. et al.**, A humanized mouse identifies the bone marrow as a niche with low therapeutic IgG activity. *Cell Rep.* 2014. **7**: 236–248.

24 **Katano, I., Ito, R., Kawai, K. and Takahashi, T.**, Improved detection of in vivo human NK cell-mediated antibody-dependent cellular cytotoxicity using a novel NOG-FcγR-deficient human IL-15 transgenic mouse. *Front. Immunol.* 2020. **11**: 532684.

25 **Takai, T., Li, M., Sylvestre, D., Clynes, R. and Ravetch, J. V.**, FcR γ chain deletion results in pleiotrophic effector cell defects. *Cell* 1994. **76**: 519–529.

26 **Nimmerjahn, F., Bruhns, P., Horiuchi, K. and Ravetch, J. V.**, FcγRIV: a novel FcR with distinct igg subclass specificity. *Immunity* 2005. **23**: 41–51.

27 **Beutier, H., Gillis, C. M., Iannascoli, B., Godon, O., England, P., Sibilano, R., Reber, L. L. et al.**, IgG subclasses determine pathways of anaphylaxis in mice. *J. Allergy Clin. Immunol.* 2017. **139**: 269–280.e7.

28 **Strowig, T., Gurer, C., Ploss, A., Liu, Y.-F., Arrey, F., Sashihara, J., Koo, G. et al.**, Priming of protective T cell responses against virus-induced tumors

in mice with human immune system components. *J. Exp. Med.* 2009. **206**: 1423–1434.

29 **Chijioke, O., Müller, A., Feederle, R., Barros, M. H. M., Krieg, C., Emmel, V., Marcenaro, E. et al.**, Human natural killer cells prevent infectious mononucleosis features by targeting lytic Epstein-Barr virus infection. *Cell Rep.* 2013. **5**: 1489–1498.

30 **Leatherbarrow, R. J. and Dwek, R. A.**, Binding of complement subcomponent Clq to mouse IgGl, IgG2a AND IgG2b: A novel Clq binding assay. *Mol. Immunol.* 1984. **21**: 321–327.

31 **Terry, L. A., DiSanto, J. P., Small, T. N. and Flomenberg, N.**, Differential expression and regulation of the human CD8α and CD8β chains. *Tissue Antigens* 1990. **35**: 82–91.

32 **Peschke, B., Keller, C. W., Weber, P., Quast, I. and Lünemann, J. D.**, Fc-galactosylation of human immunoglobulin gamma isotypes improves C1q binding and enhances complement-dependent cytotoxicity. *Front. Immunol.* 2017. **8**: 646.

33 **de Taeye, S. W., Bentlage, A. E. H., Mebius, M. M., Meesters, J. I., Lissenberg-Thunnissen, S., Falck, D., Sénard, T. et al.**, FcγR binding and ADCC activity of human IgG allotypes. *Front. Immunol.* 2020. **11**: 740.

34 **Steplewski, Z., Sun, L. K., Shearman, C. W., Ghrayeb, J., Daddona, P. and Koprowski, H.**, Biological activity of human-mouse IgG1, IgG2, IgG3, and IgG4 chimeric monoclonal antibodies with antitumor specificity. *Proc. Natl. Acad. Sci. USA* 1988. **85**: 4852–4856.

35 **Tao, M. H., Smith, R. I. and Morrison, S. L.**, Structural features of human immunoglobulin G that determine isotype-specific differences in complement activation. *J. Exp. Med.* 1993. **178**: 661–667.

36 **Brüggemann, M., Williams, G. T., Bindon, C. I., Clark, M. R., Walker, M. R., Jefferis, R., Waldmann, H. et al.**, Comparison of the effector functions of human immunoglobulins using a matched set of chimeric antibodies. *J. Exp. Med.* 1987. **166**: 1351–1361.

37 **Derebe, M. G., Nanjunda, R. K., Gilliland, G. L., Lacy, E. R. and Chiu, M. L.**, Human IgG subclass cross-species reactivity to mouse and cynomolgus monkey Fcγ receptors. *Immunol. Lett.* 2018. **197**: 1–8.

38 **Dekkers, G., Bentlage, A. E. H., Stegmann, T. C., Howie, H. L., Lissenberg-Thunnissen, S., Zimring, J., Rispens, T. et al.**, Affinity of human IgG subclasses to mouse Fc gamma receptors. *mAbs* 2017. **9**: 767–773.

39 **Hezareh, M., Hessell, A. J., Jensen, R. C., van de Winkel, J. G. and Parren, P. W.**, Effector function activities of a panel of mutants of a broadly neutralizing antibody against human immunodeficiency virus type 1. *J. Virol.* 2001. **75**: 12161–12168.

40 **Huntington, N. D., Legrand, N., Alves, N. L., Jaron, B., Weijer, K., Plet, A., Corcuff, E. et al.**, IL-15 trans-presentation promotes human NK cell development and differentiation in vivo. *J. Exp. Med.* 2009. **206**: 25–34.

41 **Titus, J. A., Perez, P., Kaubisch, A., Garrido, M. A. and Segal, D. M.**, Human K/natural killer cells targeted with hetero-cross-linked antibodies specifically lyse tumor cells in vitro and prevent tumor growth in vivo. *J. Immunol.* 1987. **139**: 3153–3158.

42 **Anderson, C. L., Shen, L., Eicher, D. M., Wewers, M. D. and Gill, J. K.**, Phagocytosis is mediated by three distinct Fcy receptor classes on human leukocytes. *J. Exp. Med.* 1990. **171**: 1333–1345.

43 **Clynes, R., Takechi, Y., Moroi, Y., Houghton, A. and Ravetch, J. V.**, Fc receptors are required in passive and active immunity to melanoma. *Proc. Natl. Acad. Sci. USA* 1998. **95**: 652–656.

44 **Uchida, J., Hamaguchi, Y., Oliver, J. A., Ravetch, J. V., Poe, J. C., Haas, K. M. and Tedder, T. F.**, The innate mononuclear phagocyte network depletes B lymphocytes through Fc receptor–dependent mechanisms during anti-CD20 antibody immunotherapy. *J. Exp. Med.* 2004. **199**: 1659–1669.

45 **Albanesi, M., Mancardi, D. A., Jönsson, F., Iannascoli, B., Fiette, L., Di Santo, J. P., Lowell, C. A. et al.**, Neutrophils mediate antibody-induced antitumor effects in mice. *Blood* 2013. **122**: 3160–3164.

46 **Montalvao, F., Garcia, Z., Celli, S., Breart, B., Deguine, J., Van Rooijen, N. and Bousso, P.**, The mechanism of anti-CD20–mediated B cell depletion revealed by intravital imaging. *J. Clin. Invest.* 2013. **123**: 5098–5103.

47 **Schwab, I., Lux, A. and Nimmerjahn, F.**, Pathways responsible for human autoantibody and therapeutic intravenous IgG activity in humanized mice. *Cell Rep.* 2015. **13**: 610–620.

48 **Katano, I., Hanazawa, A., Otsuka, I., Yamaguchi, T., Mochizuki, M., Kawai, K., Ito, R. et al.**, Development of a novel humanized mouse model for improved evaluation of in vivo anti-cancer effects of anti-PD-1 antibody. *Sci. Rep.* 2021. **11**: 21087.

49 **Czajkowsky, D. M., Hu, J., Shao, Z. and Pleass, R. J.**, Fc-fusion proteins: new developments and future perspectives. *EMBO Mol. Med.* 2012. **4**: 1015–1028.

50 **Lopez-Lastra, S., Masse-Ranson, G., Fiquet, O., Darche, S., Serafini, N., Li, Y., Dusséaux, M. et al.**, A functional DC cross talk promotes human ILC homeostasis in humanized mice. *Blood Adv.* 2017. **1**: 601–614.

51 **Haeussler, M., Schönig, K., Eckert, H., Eschstruth, A., Mianné, J., Renaud, J-B., Schneider-Maunoury, S. et al.**, Evaluation of off-target and on-target scoring algorithms and integration into the guide RNA selection tool CRISPOR. *Genome Biol.* 2016. **17**: 148.

52 **Ran, F. A., Hsu, P. D., Wright, J., Agarwala, V., Scott, D. A. and Zhang, F.**, Genome engineering using the CRISPR-Cas9 system. *Nat. Protoc.* 2013. **8**: 2281–2308.

53 **Mashiko, D., Fujihara, Y., Satouh, Y., Miyata, H., Isotani, A. and Ikawa, M.**, Generation of mutant mice by pronuclear injection of circular plasmid expressing Cas9 and single guided RNA. *Sci. Rep.* 2013. **3**: 3355.

54 **Cossarizza, A., Chang, H-D., Radbruch, A., Abrignani, S., Addo, R., Akdis, M., Andrä, I. et al.**, Guidelines for the use of flow cytometry and cell sorting in immunological studies (third edition). *Eur. J. Immunol.* 2021. **51**: 2708–3145.

55 **Li, Y., Masse-Ranson, G., Garcia, Z., Bruel, T., Kök, A., Strick-Marchand, H., Jouvion, G. et al.**, A human immune system mouse model with robust lymph node development. *Nat. Methods* 2018. **15**: 623–630.

56 **Silva, J.-P., Vetterlein, O., Jose, J., Peters, S. and Kirby, H.**, The S228P mutation prevents in vivo and in vitro IgG4 Fab-arm exchange as demonstrated using a combination of novel quantitative immunoassays and physiological matrix preparation. *J. Biol. Chem.* 2015. **290**: 5462–5469.

Abbreviations: **CDC**: complement-dependent cytotoxicity · **Tx mAbs**: Therapeutic mAbs · **ADCC**: antibody-dependent cellular cytotoxicity · **ADCP**: antibody-dependent cellular phagocytosis

Full correspondence: Prof. James P. Di Santo, Innate Immunity Unit, Inserm U1223, Institut Pasteur, 25 rue du Docteur Roux, 75724 Paris, France
e-mail: james.di-santo@pasteur.fr

Received: 26/2/2023
Revised: 21/7/2023
Accepted: 21/8/2023
Accepted article online: 25/8/2023